

# An *Aplysia* cell adhesion molecule associated with site-directed actin filament assembly in neuronal growth cones

Corey Thompson<sup>1</sup>, Chi-Hung Lin<sup>2</sup> and Paul Forscher<sup>3,\*</sup>

<sup>1</sup>Department of Cell Biology, Yale University, New Haven CT 06510, USA

<sup>2</sup>Department of Microbiology and Immunology, National Yang-Ming University, Taipei, Taiwan 112, USA

<sup>3</sup>Department of Biology, Yale University, New Haven CT 06511, USA

\*Author for correspondence

## SUMMARY

During neuronal growth cone-target interactions, a programmed sequence of cytoskeletal remodeling has been described, involving increased actin assembly at the target site and directed microtubule extension into it. The cell adhesion protein apCAM rapidly accumulates at such interaction sites, suggesting a possible role in regulating cytoskeletal remodeling. To test this hypothesis we crosslinked apCAM to varying degrees with antibodies. Secondary immunocomplexes exhibited a classical patching and capping response; in contrast, high density crosslinking of apCAM by antibody coated beads triggered localized actin assembly accompanied by formation of tail-like actin structures referred to as inductopodia. When beads were derivatized with increasing amounts of anti-apCAM they displayed three sequential dose-dependent

kinetic states after binding: (1) lateral diffusion in the plane of the membrane; (2) restricted diffusion due to coupling with underlying F-actin; and (3) translocation in the plane of the membrane driven by de novo actin filament assembly local to bead binding sites, i.e. inductopodia formation. In contrast, lectin coated beads were far less efficient in triggering inductopodia formation despite demonstrated membrane protein binding. This work provides evidence that crosslinking of a diffusible membrane protein, apCAM, to threshold levels, can trigger highly localized actin filament assembly and rapid remodeling of neuronal cytoarchitecture.

Key words: Actin, Cytoskeleton, CAM (cell adhesion molecule), Neuron

## INTRODUCTION

Because of their specific homophilic and heterophilic binding properties, cell adhesion molecules, such as integrins, cadherins and the immunoglobulin superfamily of cell adhesion molecules (IgCAMs), have historically been ascribed a relatively passive role in cell-cell and cell-substrate recognition and adherence processes. Recent studies suggest, however, that adhesion molecules do much more than provide passive molecular glue and in fact may act as signaling agents, capable of actively responding to extracellular stimuli (Bixby and Harris, 1991; Neugebauer et al., 1988). In neurons, for example, IgCAMs and cadherins (Harrelson and Goodman, 1988; Doherty et al., 1991; Neugebauer et al., 1988) have been shown to act through several signal transduction pathways (Doherty et al., 1992; Atashi et al., 1992) that affect ion channel activity (Doherty et al., 1991) as well as neurite outgrowth related motility (Doherty et al., 1990a, 1991; Lemmon et al., 1989). The emerging multifunctional nature of adhesion molecules as hybrid signaling and 'adhesion' molecules is particularly intriguing with respect to the developmental problem of axonal guidance, since growth cones appear to articulate pathfinding decisions by coordinating the recognition of extracellular molecular signals with dynamic changes in cytoskeletal structure and motility (Letourneau,

1987; Letourneau et al., 1987; Lin et al., 1994; Lin and Forscher, 1995). In this report, we examine properties of apCAM, the apparent *Aplysia* homologue of NCAM, that suggest this adhesion protein could act as both adhesion protein and morphoregulatory agent.

We have previously shown that *Aplysia* bag cell neurons undergo growth cone-target interactions in vitro that involve stereotypic changes in growth cone motility and cytoskeletal structure (Lin and Forscher, 1993). During such an interaction marked changes in actin based lamellar motility occur including increased ruffling at target interaction sites and increased rates of leading edge advance, accompanied by proportional decreases in rates of retrograde F-actin flow (Lin and Forscher, 1995). Several lines of evidence now indicate that association between adhesion-like proteins and the cytoskeleton may be involved in these target recognition events and subsequent accelerated rates of neurite outgrowth (Tanaka and Sabry, 1995; Lin et al. 1994; Doherty et al., 1991). Cadherins have been shown to interact with the cytoskeleton in non-neuronal systems (Wheelock and Knudsen, 1991a,b) and within the IgCAM superfamily, NCAM (neural cell adhesion molecule) has been reported to bind the spectrin cytoskeleton (Pollerberg et al., 1986, 1987), although this result has been controversial (Hall et al., 1990). Finally, several NCAM related proteins have recently been shown to associate with spectrin,

through ankyrin linkages (Carpen et al., 1992; Davis et al., 1993).

ApCAM, an *Aplysia* IgCAM superfamily molecule, was originally identified as a glycoprotein localized to sites of neuron-neuron contacts (Keller and Schacher, 1990). apCAM has been implicated in neurite fasciculation, synaptogenesis and synaptic plasticity (Peter et al., 1994; Zhu et al., 1995; Bailey et al., 1992). Cloning showed it to be a member of the immunoglobulin superfamily, closely related to several well characterized adhesion molecules (Mayford et al., 1992). apCAM has a motif structure homologous to NCAM and fasciclin II, containing 5 extracellular immunoglobulin repeats and 2 fibronectin repeats. Sequence and western blot analysis both suggest that apCAM has multiple splice forms analogous to NCAM, including two putative glycosylphosphatidylinositol (GPI) anchored isoforms. Interestingly, we found that apCAM rapidly accumulated at sites of extensive actin remodeling during growth cone target interactions (see Fig. 1).

In a previous report, we demonstrated that attachment of highly charged polycationic beads to the peripheral lamellae of *Aplysia* bag cell neuron growth cones could trigger bursts of actin filament polymerization localized to bead-membrane binding sites, accompanied by lateral bead translocation. Our results suggested that actin assembly was generating the force to propel the beads in the plane of the membrane (Forscher et al., 1992). Beads exhibited sustained movements with apparently random trajectories forming comet shaped F-actin tails behind them dubbed 'inductopodia'. We hypothesized that the polycationic beads were recruiting membrane receptor protein(s) into complexes competent to nucleate focal actin assembly; however the identity of the proteins involved and the physiological significance of these events was unclear.

In order to investigate whether the accumulation of apCAM during growth cone target interactions could be responsible for the observed effects on actin dynamics, we used bead pseudo-targets derivatized with a monoclonal anti-apCAM antibody (4E8) to directly crosslink apCAM to various degrees. We show that high density crosslinking of apCAM is sufficient to induce site-directed actin polymerization and the accompanying formation of inductopodia. The behavior of beads bound to apCAM depended critically on the level of crosslinking, suggesting that this membrane protein may interact with the cytoskeleton in multiple ways depending on its physiological state. We hypothesize that apCAM may serve a dual role in growth cones: as an adhesion molecule, as shown previously (Keller and Schacher, 1990), and as a morphoregulatory receptor, responding to extracellular cues by inducing cytoskeletal changes.

## MATERIALS AND METHODS

### Cell culture

Dissociated bag cells from 100-150 g *Aplysia californica* (Marinus Inc., Long Beach, CA) were plated onto poly-L-lysine coated coverslips in serum-free L-15 medium supplemented with seawater salts as described previously (Forscher et al., 1987). Experiments were done in laminar flow chambers, and perfused at 22°C with artificial seawater (ASW) buffer containing (mM): 400 NaCl, 10 KCl, 10 CaCl<sub>2</sub>, 55 MgCl<sub>2</sub>, 15 HEPES at pH 7.8.

### Microscopy and image processing

Light microscopy and image processing was done essentially as

described (Forscher and Smith, 1988). Bead centroid positions were calculated every 33 milliseconds (every video frame) using software developed for a 151-AT series image processor (Imaging Tech., Bedford, MA). A binary threshold LUT was used to isolate areas occupied by beads. Centroid positions were then calculated as the average  $x$  and  $y$  coordinates of bead areas.

For real time analysis, cells were imaged with a Newvicon camera (Hamamatsu, Middlesex, NJ) and background-subtracted video sequences were recorded onto S-VHS tape. Diffusion analysis was done essentially as by Qian et al. (1991) and Sheetz et al. (1989). Briefly, particle centroid positions were measured using 33 millisecond (video frame rate) sampling intervals for 450 frames. To calculate the diffusion coefficients ( $D$ ), periods of bead motility approximately 15 seconds long were analyzed. The mean particle displacement (MSD) was calculated using intervals ranging from 0.033-1 second long, for the extent of the beads' voyage. The ensemble averages of such MSDs were then plotted versus the time interval. This curve was then fitted to the diffusion equation  $\langle x^2 \rangle = 4Dt + v^2 t^2$  (using Excel v7.0), the coefficients yielding both  $D$  and velocity ( $v$ ). Doing so resulted in a maximum error of ~20% at the longest time interval used, given that the relative error of  $\langle x^2 \rangle$  at time  $t$  is  $0.82(N/n)^{-1/2}$ , where  $N$  is the total number of time points (450), and  $n$  is the largest time interval (30). When a diffusion coefficient was calculated for a control bead bound to the poly-L-lysine coverslip, a  $D$  with no drift component and about 2 orders of magnitude lower than the smallest experimental  $D$  was obtained (see Results and Table 2).

### Fluorescence analysis

Fixation of cells under video observation was done essentially as described previously (Forscher and Smith, 1988). Cells were permeabilized using 100 µg/ml saponin in fixation buffer (4% paraformaldehyde in ASW, 400 mM sucrose) for 5 minutes, and washed with PBS after extraction. Rhodamine-phalloidin (Molecular Probes, Eugene, OR) was used at 1 unit/ml, and 4E8 at 5-15 µg/ml in PBS, and FITC-conjugated goat anti-mouse (Jackson Labs, West Grove, PA) was used as a secondary antibody. To examine the behavior of apCAM crosslinked by monoclonal antibody alone, cells were treated with 4E8 for 5 minutes, washed with ASW and incubated for 60 minutes, then fixed. 4E8 localization was then determined by immunofluorescence staining with a secondary antibody. For patching and capping studies, cells were primed with 4E8 as described above, then exposed to FITC-conjugated goat anti-mouse antibody that had been dialyzed overnight against ASW at a concentration of 5 µg/ml. After varying amounts of time (1-10 minutes), cells were fixed, extracted and stained with rhodamine-phalloidin as above. For dynamic analysis of patching and capping, cells were treated with 4E8 and secondary antibody as above, and time lapse sequences were obtained using a SIT camera (Hamamatsu, Middlesex, NJ).

### Laser diode optical trap

An IR laser trap was constructed for use in these studies using a simple optical design similar to those described previously (Block, 1990; Svoboda and Block, 1994). A 40 mW laser diode emitting at 830 nm (Sharp LT015MD0, Osaka, Japan) was used. A peltier device maintained the laser diode case at 12-15°C. The output beam was collimated (Rodenstock Precision Optics Inc., Rockford, IL), circularized with an anamorphic prism pair (Melles Griot, Irvine, CA) and directed into a 1.25× beam expanding telescope also used for beam steering. The 2FL fluorescence housing from a Zeiss Axiovert 10 microscope was modified to incorporate a short pass dichroic mirror (780 nm; Chroma Tech, Burlington, VT). A 100×/1.25 Zeiss Neofluar objective was used in trapping experiments.

### Bead derivatization

Polyethyleneimine (PE) beads were prepared as previously reported (Forscher and Smith, 1990). Polystyrene beads (300 nm diameter; Interfacial Dynamics Co., Portland, OR) derivatized with recombinant

Protein A/G were used in initial antibody linking (see Fig. 2) and low antibody dose priming studies (see Fig. 8). To prime cell surfaces for use with Protein A/G beads, anti-apCAM monoclonal antibody 4E8 (a generous gift from Drs Flavio Keller and Sam Schacher) was diluted in ASW to a final concentration of either 0.05 µg/ml or 1-3 µg/ml for low and high level antibody treatments, respectively. The antibody solution was added to the perfusion chamber for 5 minutes under DIC observation and then washed out by ASW perfusion. For laser trapping studies, glutaraldehyde activated beads were prepared from silica beads (800 nm diameter) with aminopropyl functional groups (Bangs Laboratories, Carmel, IN) as follows: a 1% (w/v) aqueous bead suspension was mixed with an equal volume of 8% EM grade glutaraldehyde (Polysciences, Warrington, PA) and incubated at 22°C for ~6 hours with gentle mixing, gently pelleted and resuspended 3× in 25 mM Na-phosphate buffer, pH 7.0, at 1% (w/v) beads and used directly for protein coupling or stored at 4°C. Glutaraldehyde activated beads were derivatized with avidin or Protein A/G and used for biotinylated lectins (see Fig. 6) or antibody studies (see Fig. 7), respectively, as described below. A 1% solids bead stock solution was generally diluted 250- to 1,000-fold in ASW before addition to cells.

### Protein-bead coupling

Recombinant Protein A/G (Calbiochem, La Jolla, CA), or Avidin-D (Vector Laboratories, Burlingame, CA) was added to the glutaraldehyde activated bead suspension at 200-400 µg/ml protein in 25 mM Na-phosphate buffer, pH 7.0, and mixed gently for at least 4 hours at 22°C. Protein coupled beads were then pelleted and resuspended 3× in 50 mM Tris buffer, pH 8, and 1% bovine serum albumen was added to backfill any residual crosslinking sites. Protein linked beads were stored at 4°C. Protein A/G-conjugated silica beads were incubated with 4E8 at 500 µg/ml for 20 minutes, and washed prior to use, when used directly. Bead concentrations for laser trapping experiments were determined empirically.

### Lectin-bead linkage

Avidin silica beads (800 nm diameter) were incubated with biotinylated lectins (Vector Laboratories) at 1 mg/ml for 30 minutes, then pelleted and resuspended 3× in 10 mM Tris-HCl, pH 8. Each biotinylated lectin bead lot was tested for lectin adsorption prior to use by incubating an aliquot of the beads with FITC-conjugated Avidin-D (Vector Laboratories) at 5 µg/ml for 20 minutes, washing in Tris buffer, then observing under epifluorescence. Beads with attached lectins fluoresced under FITC excitation, while control avidin beads did not. Lectin beads were applied to the cell surface using the laser trap, and behavior was scored essentially as described above for antibody linked beads.

### 4E8 dilution beads

A single lot of Protein A/G beads (800 nm diameter), made as above, was incubated overnight with a 1 mg/ml mixture of 4E8 and a nonimmune IgG of the same subclass (IgG2a), RPC5 (Cappel, Durham, NC), with 4E8 comprising either 10%, 50%, 75% or 100% of the total. Free antibody was washed away just prior to experiments. Beads were always stored in antibody solutions when not in use. Beads were placed and held against the cell surface for 10 seconds using the laser trap. Beads known to form inductopodia were applied at the end of each experiment, and only those cells capable of forming any inductopodia were used for statistical analysis. Antibody binding capacity was assessed by incubating Protein A/G beads with 1 mg/ml RPC5, then quantitating antibody bound by scanning densitometry of Coomassie stained gels, using known RPC5 concentrations as calibration standards. Binding capacity was 7,400 IgG molecules per 800 nm bead, or 3,700 molecules/µm<sup>2</sup>.

### Protein blots

*Aplysia* nervous system membrane proteins were enriched essentially as reported previously (Keller and Schacher, 1990). Briefly, all

ganglia and connectives from 3 animals were homogenized thoroughly in buffer (250 mM sucrose, 25 mM Tris-HCl, 3 mM EDTA, 1 mM EGTA, 0.5 mM Pefabloc (Boehringer Mannheim, Indianapolis, IN), pH 7.5, spun 10 minutes at 1,600 g. The supernatant was spun at 150,000 g for 3 hours. Pelleted membranes were resuspended overnight in buffer (150 mM NaCl, 25 mM Tris-HCl, 2.5% Triton X-100, 0.5 mM pefabloc, pH 7.5). The resulting extract was clarified at 150,000 g for 1 hour. This membrane extract was boiled in 10× SDS sample buffer (20% SDS, 1 M DTT, 600 mM Tris-HCl, 0.01% bromophenol blue, pH 6.8), and run on a 10% gel by standard SDS-PAGE. Separated proteins were then transferred to 0.2 µm nitrocellulose (Schleicher and Schuell, Keene, NH). The nitrocellulose was cut into strips and blocked with TBS/Tw20 (137 mM NaCl, 3 mM KCl, 25 mM Tris-HCl, pH 8.0 (TBS) + 0.1% Tween-20) for 45 minutes. Endogenous biotinylated proteins were blocked using an Avidin/biotin blocking kit (Vector). Biotinylated lectins (Vector) were then added at 10 µg/ml for 30 minutes in TBS/Tw20. The strips were then washed 3× with TBS/Tw20, and incubated with 0.2 units/ml avidin-conjugated alkaline phosphatase (Vector) in TBS/Tw20 for 30 minutes. After washing, the blot was developed by standard techniques.

### Lectin precipitations

Avidin-D agarose (Vector) was washed thoroughly in TBS/Ca (TBS + 1 mM CaCl<sub>2</sub>). 200 µg/ml biotinylated lectin (Vector) was then bound to the agarose, washed in TBS/Ca, then added to *Aplysia* membrane extract, made as described above. For ConA sugar competition, methyl α-manno-pyranoside (E-Y Labs, San Mateo, CA) was added to the extract at 200 mM prior to adding ConA agarose. After incubation for 1 hour, the agarose was separated from the membrane extract supernatant. Both supernatant and pellet were mixed with 10× SDS sample buffer, boiled, run on a 5-16% gradient polyacrylamide gel, then transferred to 0.2 µm nitrocellulose, blocked with 5% dry milk in TBS/Tw20 for 90 minutes, incubated overnight with 4E8 at 5 µg/ml in the presence of blocker, washed, incubated with alkaline phosphatase-conjugated secondary (Promega, Madison, WI) at 0.133 µg/ml for 1-3 hours, then developed by standard techniques. Unless otherwise noted, all chemicals were obtained from Sigma (St Louis, MO).

## RESULTS

### apCAM accumulates at sites of active actin assembly

Two growth cones were allowed to interact as described previously (Lin and Forscher, 1993): membrane ruffling occurred at the site of contact (Fig. 1B, arrowhead), accompanied by extension of the central microtubule rich domain along the interaction axis (Fig. 1A and B, arrows). Addition of a soluble monoclonal anti-apCAM antibody (4E8) known to recognize an extracellular epitope of apCAM has been a useful inhibitor of adhesion in previous studies (Keller and Schacher, 1990) and not surprisingly, we found that 4E8 also inhibited growth cone-target interactions like the one shown in Fig. 1 (data not shown). When apCAM was localized in interacting growth cones, a striking accumulation was observed at the target interaction site in domains of lamellipodial overlap (Fig. 1C,D), concomitant with very high levels of actin assembly, protrusive activity and ruffling (Lin and Forscher, 1993). ApCAM immunofluorescence at that target interaction site was greater than the sum of the staining intensities of the two overlapping growth lamellae (Fig. 1E), indicating true accumulation. As a result of these observations, we were prompted to investigate a potential role for apCAM in regulating actin assembly.

### apCAM crosslinking is sufficient to induce actin assembly

Experiments were designed to examine the effects of crosslinking apCAM with bead 'pseudotarget' substrates on growth cone motility and structure. Bag cell neurons were treated for 5 minutes with 1-3  $\mu\text{g/ml}$  4E8 to prime the cell surface. Cells were then perfused with ASW to wash out unbound antibody, after which polystyrene beads derivatized with Protein A/G (300 nm) were added to the system. When beads landed on growth cone lamellae, they bound 4E8-apCAM and quickly became passively coupled to the retrograde F-actin flow (Forscher and Smith, 1990; Lin and Forscher, 1993). After a variable delay, most beads began to exhibit active motility, independent of the retrograde flow, characterized by formation of distinct tail-like structures behind beads as they moved on the membrane surface (Fig. 2A,C). These structures were composed of F-actin, as evidenced by rhodamine-phalloidin staining (Fig. 2A,B, arrowheads).

The morphological features of these structures are essentially indistinguishable from those reported in our initial characterization of 'inductopodia' (Forscher et al., 1992). However, while inductopodia triggered by polycationic beads were inhibited by addition of extracellular blocking proteins, inductopodia triggered by apCAM crosslinking were not affected by high concentrations of added BSA (>5 mg/ml). In

addition, inductopodia triggered by apCAM crosslinking occurred more frequently and were longer-lived than those induced by polycationic beads (data not shown). Note that the inductopodium shown in the time course depicted in Fig. 2C is moving 'upstream' against the retrograde F-actin flow (black arrow indicates flow direction) during the first part of the sequence. Cells that did not receive 4E8 priming exhibited low affinity for Protein A/G beads.

### Monoclonal antibody treatment alone does not change apCAM distribution

Based on the above observations, we hypothesized that inductopodia formation might be triggered by localized, multivalent crosslinking of apCAM via antibody interactions with Protein A/G beads. To test this hypothesis, we looked at apCAM and F-actin distributions in growth cones under conditions of increasing degrees of apCAM crosslinking.

To determine whether the 4E8 priming treatment *alone* might be perturbing the normal distribution of apCAM and F-actin, both of these proteins were localized by immunofluorescence in untreated cells and compared with cells previously exposed to 4E8. In untreated cells and compared with cells previously exposed to 4E8, apCAM had a homogeneous distribution on the growth cone surface (Fig. 3A), in agreement with previous reports (Keller and Schacher, 1990; Mayford et al., 1992). The F-actin

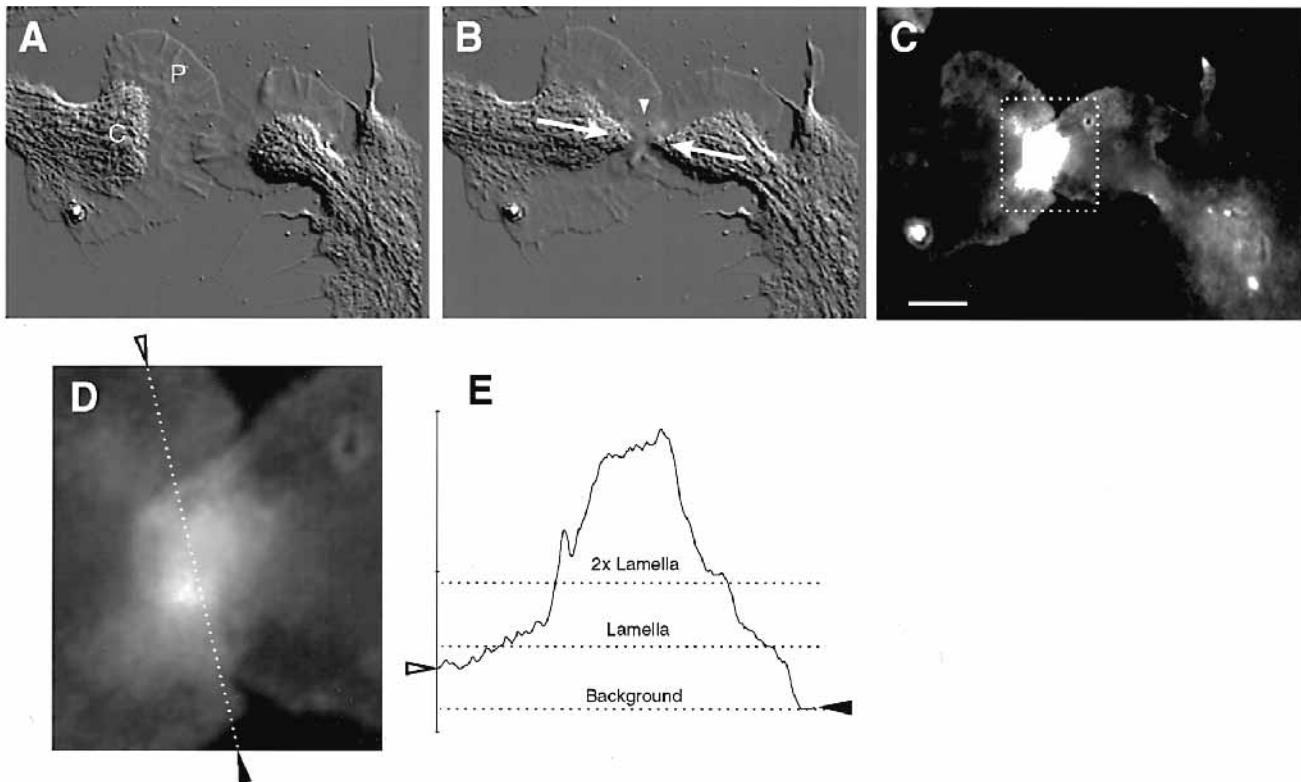


**Fig. 1.** apCAM is concentrated at sites of growth cone-target interactions. (A) DIC image of cells 20 minutes after initial contact, but before cytoskeletal remodeling associated with interaction, demonstrating the peripheral (P) and central (C) domains of a control growth cone. (B) 27 minutes after initial contact, the growth cones demonstrate a typical interaction: central domains extend towards the site of contact (arrows), and actin ruffling occurs at the contact site (arrowhead). (C) Immunofluorescent staining with 4E8 shows apCAM is concentrated at the interaction site (box). Image has been intensified to clearly show apCAM distribution in non-overlapping regions. (D) Magnified view of interaction site (box in C), showing detail of 4E8 staining. (E) Intensity profile along dotted line in D, showing relative intensities of background, single lamella, and expected intensity of 2 overlapping lamellae. Note that apCAM staining intensity exceeds that expected from simple overlap. Open and closed arrowheads in D correspond to those in E. Bar, 5  $\mu\text{m}$ .

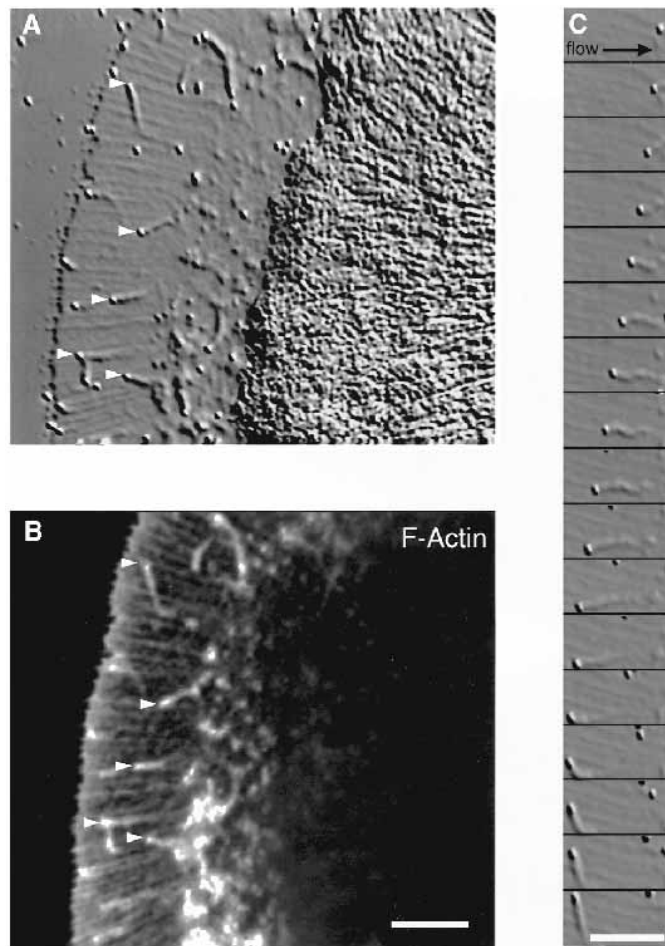


**Fig. 2.** Local apCAM crosslinking by solid phase substrate triggers actin assembly. A growth cone lamella coated with monoclonal antibody to apCAM was treated with Protein A/G beads. Beads adhered tightly to cells, and induced actin assembly at the binding site, forming inductopodia. (A) Video-DIC image of inductopodia (arrowheads) triggered on a growth cone lamella treated as above. (B) Rhodamine-phalloidin stain of same field demonstrating F-actin localization to inductopodia tails, and regions of active actin ruffling. (C) Time course of inductopodium growth; each frame = 10 seconds. The inductopodium followed in C is marked with the uppermost white arrowhead in A and B. Black arrow in C shows direction of retrograde flow. Bars, 10  $\mu$ m.

distribution for the same field is shown in Fig. 3B. To examine possible effects of prolonged 4E8 antibody treatment, live cells were first primed with 4E8 (1–3  $\mu$ g/ml) for 5 minutes; then, after washing out unbound antibody, the cells were incubated at 22°C for 1 hour. These cells were then fixed, lightly permeabilized, and stained for membrane bound 4E8 and F-actin. The resulting pattern of apCAM (4E8) and F-actin staining (Fig. 3C,D) was nearly indistinguishable from untreated cells stained after fixation (Fig. 3A,B). Note that there was no evidence of apCAM capping induced by the long term 4E8 treatment alone (Fig. 3C). Somewhat decreased levels of cell surface staining (relative to post-fixation 4E8 staining) were observed when live cells were treated with 4E8. This difference is likely due to the reduced affinity of the 4E8 antibody for its antigen in the high salt levels present in artificial seawater. To demonstrate that the

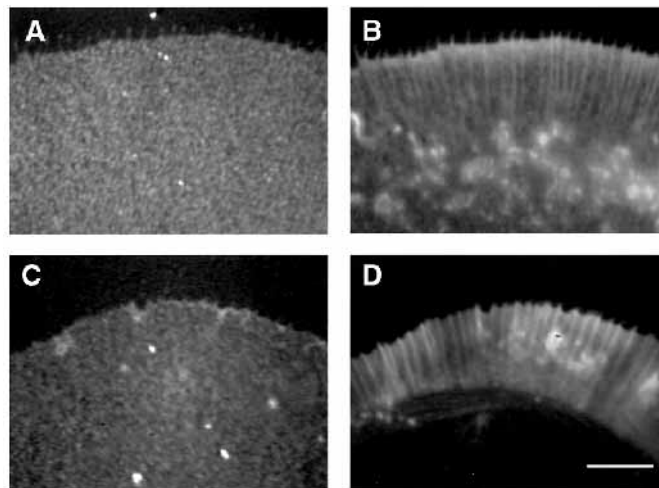


**Fig. 3.** apCAM under control conditions is uniformly distributed. (A) A control growth cone lamella fixed and stained for surface apCAM, and (B) actin. (C) A live growth cone was treated with monoclonal antibody to apCAM, washed, and incubated for 60 minutes, then fixed and stained for surface IgG, and (D) actin. Staining intensities in A and C were normalized to emphasize distribution. Note that apCAM crosslinking with the monoclonal antibody did not alter actin structure, and treatment with monoclonal antibody alone did not alter apCAM surface distribution. Bar, 10  $\mu$ m.

homogeneous *pattern* of staining was maintained, image intensities in Fig. 3A and C were normalized. In summary, F-actin and apCAM distributions did not appear to be affected by the presence of the 4E8 antibody alone.

### Limited crosslinking of apCAM results in passive F-actin coupling

To test the effect of limited cross-linking of cell surface apCAM molecules, fluorescent secondary antibody-apCAM immunocomplexes were generated, and their dynamics observed in live cells. Cells were first treated briefly with 4E8 followed by FITC-conjugated goat anti-mouse IgG. The cells were then incubated with this secondary antibody for varying time intervals before fixation and staining. With increasing incubation time, apCAM tended to concentrate into patches and move in a retrograde direction (Fig. 4A,C,E,G). After a 2 minute treatment, a band cleared of fluorescence was observed near the leading edge of the growth cone (Fig. 4A, *white line* marks leading edge of cell). After 5 minutes of antibody treatment, patches were larger and more dispersed, and the region of attenuated fluorescence along the distal growth cone margin had widened (Fig. 4G). This appears similar to patching and capping, which has been described in several cell types, for many membrane proteins (Holifield et al., 1990; Holifield and Jacobson, 1991; Shiozawa et al., 1989). F-actin structure did not appear to be altered during this process (Fig. 4B,D,F,H). Areas of intense rhodamine-phalloidin staining in the proximal ‘transition zone’ region of the lamella are normal for this cell type (Forscher and Smith, 1988), and did not appear to colocalize with patches of antibody crosslinked apCAM.

The experiments in Fig. 4A–H were performed on separate cells fixed at various time points in order to observe possible changes in actin structure. To test whether the clearance of

crosslinked 4E8-antibody complexes described above represented retrograde flux of apCAM patches, growth cones were treated with 4E8 followed by fluorescent secondary antibody as above, and immune complex movement was followed by time-lapse video recording (Fig. 5). Over time apCAM patches formed and moved steadily in a retrograde direction. The pattern and rate of clearance in both of the above experiments was about 3  $\mu\text{m}/\text{minute}$ , the typical rate of F-actin flow in these growth cones (Forscher and Smith, 1988), strongly suggesting that the patches were moving by a mechanism involving passive coupling to underlying F-actin (Lin and Forscher, 1995).

#### Lectins do not trigger inductopodia as frequently as 4E8

To investigate the specificity of inductopodia formation

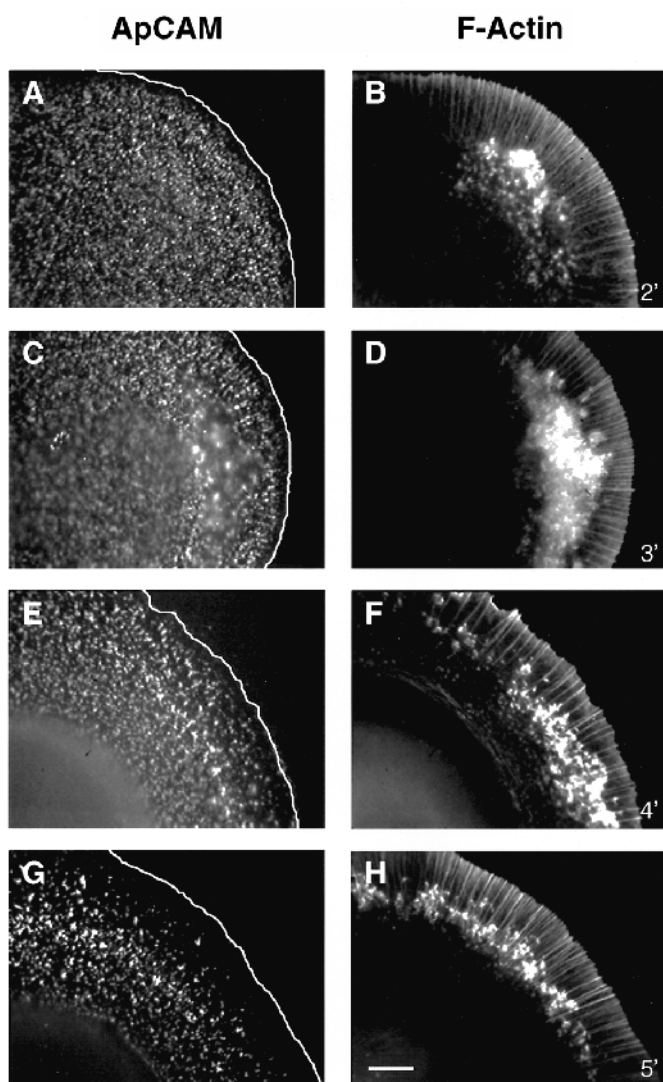


**Fig. 4.** Crosslinking apCAM with primary and secondary antibodies causes patching and capping of apCAM, but not actin reorganization. (A,C,E,G) Fluorescent images of cells which were treated with monoclonal antibody to apCAM, then with a fluorescent secondary antibody for varying amounts of time, and fixed. Time is shown in lower right. (B,D,F,H) Corresponding rhodamine-phalloidin F-actin stains of the same fields as in A,C,E,G. White lines indicate leading edges of cells. Bar, 10  $\mu\text{m}$ .

mediated by apCAM crosslinking, a battery of lectin coated beads were screened for their ability to induce site directed actin assembly. First, nitrocellulose blots of *Aplysia* nervous tissue were probed with 15 different biotinylated lectins, using avidin-labeled alkaline phosphatase as a detection method (not shown). Five lectins with contrasting protein binding profiles were chosen as membrane probes (Table 1; Fig. 6A). To test whether any of the lectins used bound apCAM, *Aplysia* CNS proteins were precipitated from a membrane extract with biotinylated lectins coupled to avidin-agarose. Precipitated proteins were separated by gel electrophoresis, transferred to nitrocellulose, and blotted with 4E8 (Fig. 6B). Of the lectins tested, only ConA exhibited significant apCAM binding. One major and two minor 4E8 immunoreactive bands were detected, in agreement with previous reports (Keller and Schacher, 1990). ConA-apCAM interactions appeared to be specific as they were competitively inhibited by inclusion of the soluble ConA substrate  $\alpha$ -manno-pyranoside (Fig. 6B, ConA/sugar).

To examine the dynamic behavior of membrane proteins bound by each lectin species in live cells, lectin-coated silica beads (800 nm diameter) were added to the perfusion chamber at low concentrations in the presence of BSA (to minimize nonspecific interactions), and applied to the surface of growth cone lamellae using a single beam gradient laser trap. Beads were held in position against the surface of the cell with the laser trap for 10 seconds before being released in order to allow membrane attachments to develop and to standardize the bead application procedure. We found that this protocol facilitated observation of low affinity lectin-membrane binding interactions that did not occur frequently when using simple diffusion mediated bead application.

After release from the laser trap, beads were categorized as being either adherent or nonadherent; the latter was operationally defined as a bead that either diffused away from the cell, or could be pulled off the membrane with the laser trap. Adherent beads were further categorized as: (1) diffusive - beads diffused or could be moved laterally in the plane of the membrane, but could not be pulled off the growth cone surface with the laser trap; or (2) flow coupled - beads showed little visible diffusion, could not be moved with the laser trap and moved in synchrony with underlying F-actin. The probability of observing each behavior was then assessed for each bead conjugate (Fig. 6C). Since beads displayed some or all of these behaviors prior to forming inductopodia, the probability of each bead conjugate forming inductopodia was calculated independently (Fig. 6D: 437 beads, 24 experiments). Avidin beads with no attached lectins and 4E8 coated Protein A/G-silica beads were used as negative and positive controls, respectively.

Since lectins rarely elicited inductopodia formation, each

**Table 1. Lectin behaviors**

Lectin	Protein species bound	% Inductopodia
<i>Sophora japonica</i> agglutinin (SJA)	~3	0
Succinyl wheat germ agglutinin (S-WGA)	~10	19
<i>Lens culinaris</i> agglutinin (LCA)	~25	4
Wheat germ agglutinin (WGA)	>25	2
Concanavalin A (ConA)	$\geq 25$	0

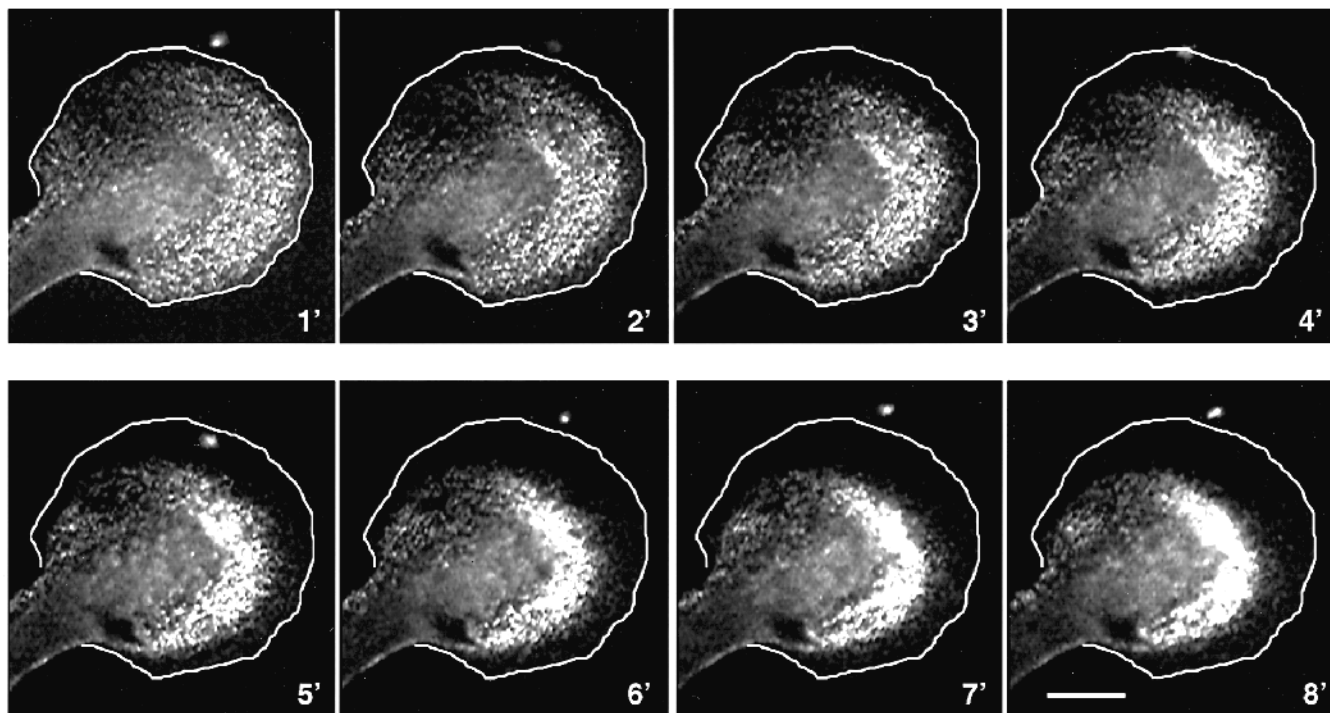


**Fig. 5.** apCAM movement during capping occurs at the rate of retrograde F-actin flow. A cell was treated with 4E8, then with fluorescent secondary antibody. Fluorescent immunocomplex distribution was followed over time by timelapse recording. White lines mark leading edge position. Time in minutes from secondary antibody addition is shown in lower right. Rate of retrograde clearance = 3  $\mu\text{m}/\text{minute}$ . Bar, 10  $\mu\text{m}$ .

cell was also tested post-experimentally for its competence to form inductopodia using either 4E8- or PE- coated silica beads, and only those cells capable of forming inductopodia were used for calculations. Of the lectins tested, only LCA, S-WGA and WGA were able to elicit inductopodia formation when bound to avidin beads; however, the probability of inductopodia formation was significantly lower (4%, 19% and 2%, respectively) than for 4E8 coated beads (83%). Interestingly, although ConA bound apCAM, and many other protein species (Fig. 6B), ConA-conjugated beads *never* formed inductopodia (Fig. 6D). These results suggested the possibility that *high density* crosslinking of apCAM may be a prerequisite to the formation of competent actin assembly sites.

#### Bead behavior as a function of apCAM crosslinking density

To investigate the relationship between bead behavior, actin assembly and apCAM crosslinking levels further, Protein A beads were prepared with varying surface densities of 4E8. This was accomplished by incubating Protein A/G derivatized silica beads (800 nm diameter) with defined concentration ratios of 4E8 in a background of RPC5, a control monoclonal antibody of the same IgG subclass as 4E8 (IgG2a). Protein A/G should bind each antibody with equal avidity, resulting in beads with fixed 4E8 to RPC5 ratios at equilibrium. Beads with 10%, 50%, 75% or 100% 4E8 bound were placed on growth cone lamellae with the laser trap, and categorized as being either adherent or nonadherent and diffusive or flow coupled and the probability of inductopodia formation assessed as above (Fig 7A: 335 beads scored,  $n=21$  experiments). The average latency time to inductopodia initiation decreased with increasing 4E8 density (Fig. 7B). Increased 4E8 surface

density also resulted in an increased probability of flow coupling (Fig. 7A,C) and inductopodia formation (Fig. 7D) for adherent beads, with a corresponding decrease in the probability of observing nonadherent or diffusing beads (Fig. 7A, right). Interestingly, although flow coupling appeared to be a roughly linear function of 4E8 surface density (i.e. apCAM crosslinking capacity) (Fig. 7C), the probability of observing inductopodia activity was a steep function of 4E8 crosslinking (Fig. 7D), suggesting threshold behavior. Beads coated with only the control antibody, RPC5, very rarely adhered to the cell surface and displayed only lateral diffusion if they bound.

#### Kinetic states may reflect progressive apCAM accumulation

To test whether the three kinetic behaviors above might be due to progressive accumulation of apCAM, cells were briefly exposed to very low concentrations of 4E8 (0.05  $\mu\text{g}/\text{ml}$ , 5 minutes), thus limiting the number of available 4E8-apCAM complexes on the cell surface. When Protein A/G derivatized polystyrene beads (300 nm diameter) were applied under these conditions, individual beads *sequentially* displayed the three types of motility described above. First, beads diffused laterally for 3-15 seconds (Fig. 8A,B; Table 2). Second, over time, beads gradually became flow coupled, exhibiting slower rates of diffusion (late time points Fig. 8B), until little or no diffusion was evident (Table 2) and beads moved in concert with retrograde F-actin flow (Fig. 8C,D; Table 2). Third, 1-5 minutes after initial membrane association, most beads formed inductopodia and began to move in the characteristic manner described previously (Fig. 8E,F; Forscher et al., 1992). Once beads formed inductopodia, they continued to exhibit restricted diffusion as judged by calculated diffusion coefficients (Table

2). Note that the calculated diffusion coefficient for a control, substrate-bound bead, was nearly two orders of magnitude less than that calculated for experimental particles (Table 2), giving us confidence that the lowest values of  $D$  reported here were indeed measurable with our system. Note that the bead shown in Fig. 8E-F exhibited a net *anterograde* displacement on the lamella as a result of inductopodia-associated movement, so it in effect moved 'upstream' against the retrograde F-actin flow. Drift (i.e. retrograde flow) components were also calculated for each phase, which correlated well with the linear velocity of the bead (Table 2).

## DISCUSSION

### Interactions with F-actin depend on apCAM crosslinking

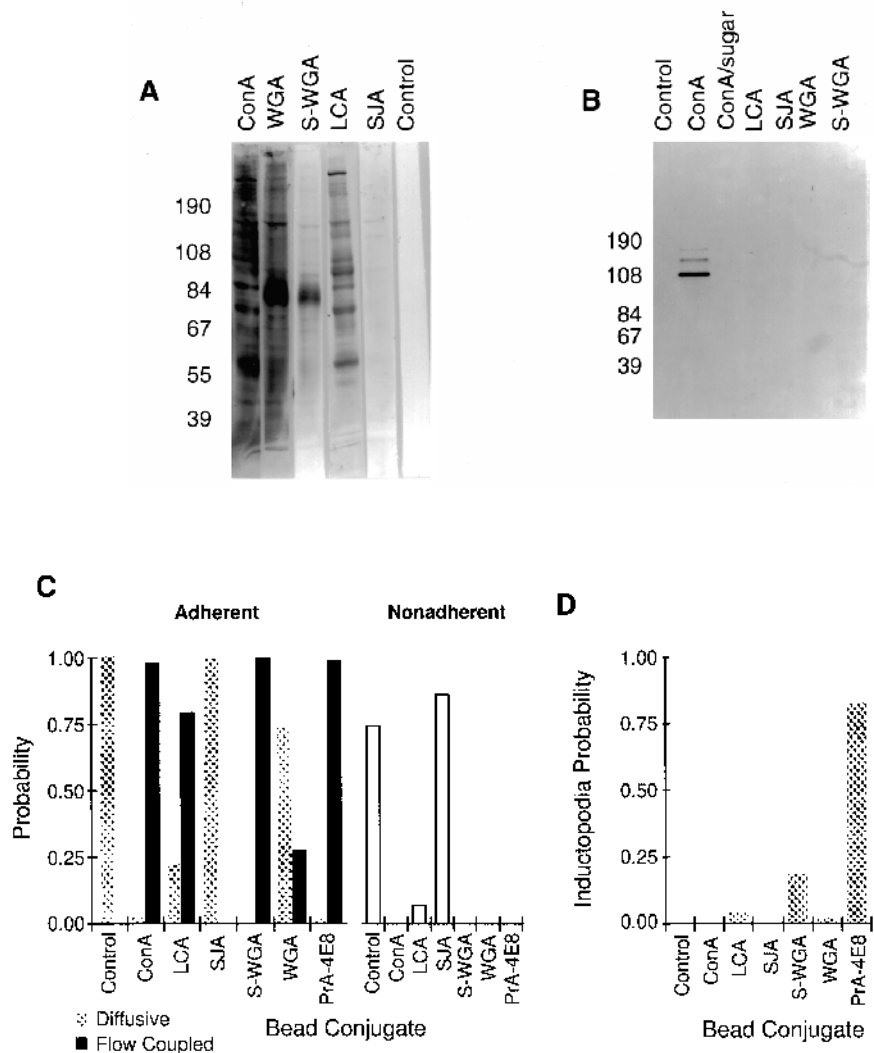
Fluorescence localization studies initially suggested that apCAM could exist in at least two states with respect to the cytoskeleton, depending upon the extent of apCAM crosslinking. Localization after fixation indicated that apCAM was distributed evenly over the surface of growth cone lamellae either under control conditions or when weakly crosslinked in living cells with 4E8, a monoclonal antibody to an extracellu-

**Table 2. Average bead diffusion coefficients**

Kinetic phase	Diffusion coefficients	
	$\pm$ s.e.m. ( $\times 10^{12}$ cm <sup>2</sup> /second)	Drift (nm/second)
Diffusive	244 $\pm$ 26.9	Undefined
Flow coupled	6.6 $\pm$ 1.6	61.4 $\pm$ 12.7
Inductopodia associated	10.7 $\pm$ 2.2	159.5 $\pm$ 37.4
Substrate bound (control)	0.075	Undefined

lar epitope of apCAM (Keller and Schacher, 1990, and Fig. 3A). When bound to 4E8 alone, apCAM maintained a homogeneous surface distribution for extended periods of time in growth cone lamellae (Fig. 3C) despite continuous retrograde flux of the underlying actin cytoskeleton (Forscher and Smith, 1988; Lin and Forscher, 1993; Lin and Forscher, 1995), suggesting that neither free apCAM nor apCAM-4E8 antibody complexes readily associate with F-actin. In contrast, when cells were treated with 4E8 followed by a fluorescent secondary antibody, the larger secondary immunocomplexes were cleared from the lamellipodium at exactly the rate of retrograde F-actin flow (Figs 4-5). This response is similar if not identical to capping of secondary immunocomplexes observed in other systems (Holifield et al., 1990; Holifield and Jacobson, 1991; Shiozawa et al., 1989). Note that the addition of a

**Fig. 6.** Lectins are poor inductopodia agonists. (A) *Aplysia* nervous system membrane extract was separated by SDS-PAGE, then blotted onto nitrocellulose. Strips of the nitrocellulose were then blotted with control solution or lectins: *Lens culinaris* agglutinin (LCA), *Sophora japonica* agglutinin (SJA), succinylated wheat germ agglutinin (S-WGA), wheat germ agglutinin (WGA), or concanavalin A (Con A). Molecular masses are shown at left (in kDa). (B) Avidin-conjugated agarose was coupled to each of the lectins listed above, then used to precipitate protein from *Aplysia* nervous system membrane extracts. Precipitated proteins were separated by SDS-PAGE, transferred to nitrocellulose, then blotted with anti-apCAM (4E8). (C) 800 nm silica beads conjugated to either avidin alone (control), Protein A/G and 4E8 (PrA-4E8) or the avidin-lectin complexes listed above, were applied to the cell surface with the optical trap for ten seconds, then released. Beads were classified as: nonadherent or adherent and diffusive or flow coupled as described in the text. For each conjugate, the probability of beads showing each behavior is plotted. (D) Probability of beads forming inductopodia is shown for each conjugate.



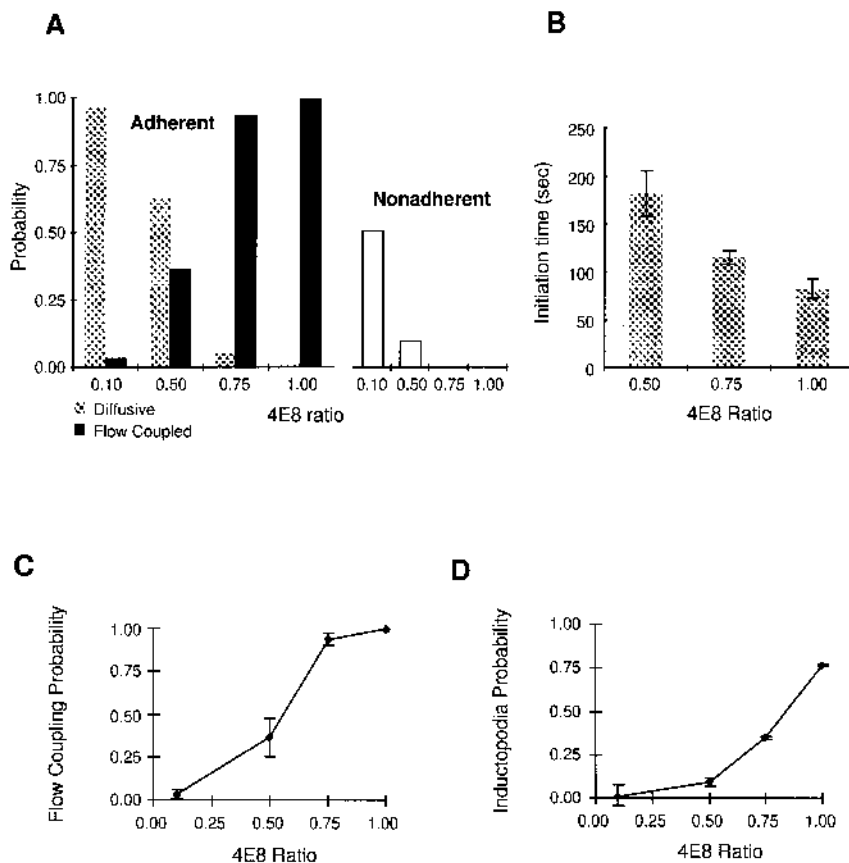


**Fig. 7.** The probability of inductopodia formation increases nonlinearly with apCAM crosslinking. (A) 800 nm Protein A/G silica beads coated with either 10%, 50%, 75% or 100% 4E8 (anti-apCAM) were applied to growth cone lamellae. Bead behavior was categorized as in Fig. 6. Plot shows probability of beads displaying each behavior. (B) Plot shows average time from initial bead-cell contact to inductopodia formation for each bead's 4E8 concentration. (C) Dose response curve showing probability of flow coupling versus relative bead 4E8 concentration. (D) Dose response curve showing probability of inductopodia formation versus bead 4E8 concentration.

secondary antibody, which would result in additional apCAM crosslinking, triggered the retrograde clearance of immunocomplexes. We also show that when cells were pretreated with limiting levels of 4E8 antibody, Protein A/G beads transitioned from an initial diffusible state to an F-actin flow coupled state over time (Fig. 8). Calculated diffusion coefficients from such beads are consistent with apCAM moving from a freely diffusible state, to one more restricted, perhaps cytoskeletally associated (Table 2). In a recent publication we demonstrated that retrograde flow-coupled beads do indeed move at exactly the same rate as underlying F-actin networks and as such can be used as noninvasive probes for studying actin filament movements in living cells (Lin and Forscher, 1995). By an independent approach, using beads coated with varying 4E8 densities, we found that increased apCAM crosslinking potential also increased the probability that freely diffusible apCAM would become coupled to the actin cytoskeleton (Fig. 7A,B).

In addition to the fairly well understood types of behavior described above, high density crosslinking of apCAM resulted in a third type of behavior - namely initiation of de novo actin assembly, and the subsequent formation of inductopodia (Figs 2, 7, 8). This third functional state appears to result from the extensive levels of apCAM crosslinking afforded by 4E8-Protein A/G bead substrates. In support, when beads were derivatized with increasing 4E8 densities, we found that the probability of inductopodia formation was a nonlinear function of apCAM crosslinking potential, i.e. actin assembly appeared to be triggered at a threshold ligand concentration (Fig. 7C).

Similarly, when Protein A/G beads were placed on cells coated with limiting bound 4E8 (Fig. 8), inductopodia growth always occurred *after* initial diffusion and coupling phases. These observations are consistent with accumulation of apCAM on the bead surface over time, by simple diffusion and trapping, leading to a transition between flow coupled and actin assembly states. Interestingly, a threshold concentration of NCAM also appears to be required to trigger neurite outgrowth (Doherty et al., 1990b), a process involving both CAM-cytoskeletal interactions and dynamic actin filament reorganization (Lin and Forscher, 1993).

### Specificity of apCAM effects

Although crosslinking of apCAM onto a solid phase bead substrate is *sufficient* to trigger site directed actin assembly, the limited number of membrane protein antibodies which cross-react with *Aplysia* proteins made it a challenge to test the relative specificity of this effect; i.e. whether crosslinking of the apCAM is necessary or if other *Aplysia* membrane proteins might also act as inductopodia agonists. For this reason, we employed lectins to address the problem of apCAM specificity. Several lectins were biochemically characterized that had unique and contrasting *Aplysia* membrane protein binding profiles. Their effects were then compared and contrasted with direct apCAM crosslinking in growth cones. Of the lectin probes tested, S-WGA, LCA and WGA coated beads were able to trigger inductopodia formation, but only at low frequencies (Fig. 6C; Table 1). Note that these lectins were much less efficient than 4E8 in eliciting actin assembly and none of them

exhibited significant apCAM binding (Fig. 6B). This suggests there may be other, albeit less efficient, routes for triggering actin assembly; for example, S-WGA, LCA or WGA could interact indirectly with apCAM or, alternatively, with effector molecules downstream of apCAM.

Some caution also needs to be exercised in interpreting the lectin binding experiments since the blots cannot discriminate between surface proteins and intracellular glycoproteins being processed. However, in this context, note that: (1) all of the lectins which bound protein on blots did in fact bind to the growth cone surface in bead experiments (Fig. 6B), suggesting the blots are at least partially representative of surface protein profiles. There is also evidence that fluorescent ConA and WGA analogs bind *Aplysia* membranes (data not shown, and Ambron et al., 1989). Finally, it is interesting to note that ConA, which bound a large number of *Aplysia* proteins including apCAM actually exhibited a *lower probability* of triggering inductopodia formation (Fig. 6C) than those lectins which bound few proteins (e.g. S-WGA, LCA). This could be explained by a necessary apCAM concentration threshold:

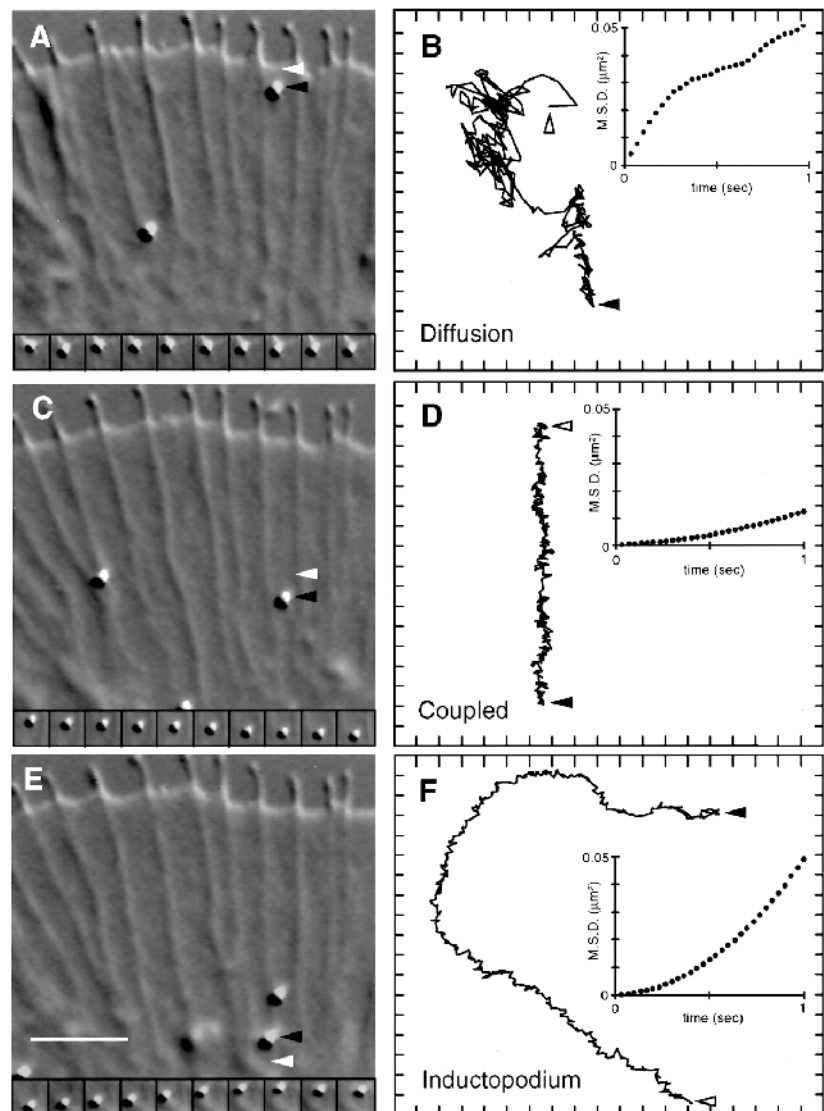
lectins binding many protein species in addition to apCAM may never achieve the requisite apCAM crosslinking density at the bead surface.

It is formally possible that the mechanism of apCAM-cytoskeleton association is not mediated by a simple concentration dependent mechanism. Although antibodies are routinely used to probe the function of membrane proteins (Holifield et al., 1990; Holifield and Jacobson, 1991; Shiozawa et al., 1989; Sheetz et al., 1990; Schmidt et al., 1995), apCAM-antibody binding could induce apCAM to interact with the actin cytoskeleton by an alternative mechanism such as ligand mediated receptor activation (Atashi et al., 1992). Physiological apCAM binding may or may not act in a similar fashion. Experiments are currently underway to test the effects of homophilic apCAM binding.

### The significance of site directed actin assembly

In this study, we attempted to mimic the physiological interaction between a growth cone and its intended target, by artificially concentrating the homophilic adhesion protein apCAM

**Fig. 8.** Three distinct kinetic states of apCAM lead to site directed actin assembly. (A,C,E) DIC images showing the bead being analyzed (start = white arrowhead; end = black arrowhead) and a time course of bead movement below each image (A, 660 msec/frame; C,E, 1,320 msec/frame). (B,D,F) Bead centroids calculated for each kinetic state using 33 milliseconds sampling intervals; tick marks are 100 nm, start and end points as above. All three phases shown are from a single bead. Mean square displacement (MSD) vs time plots are shown as insets. (A,B) Immediately after landing, bead exhibited diffusion ( $D=282 \times 10^{-12}$  cm<sup>2</sup>/second,  $v$ =undefined,  $r^2=0.9536$ ) with increasing retrograde drift. (C,D) At 1.5 minutes after landing, the bead coupled to the retrograde actin flow, and showed limited diffusion ( $D=8.9 \times 10^{-12}$  cm<sup>2</sup>/second,  $v=79.4$  nm/second,  $r^2=0.9976$ ). (E,F) At 4 minutes after contact, inductopodia formation results in bead moving to the left and anterograde against the retrograde flow and then to the right across the flow ( $D=7.6 \times 10^{-12}$  cm<sup>2</sup>/second,  $v=212$  nm/second,  $r^2=0.9997$ ). Bar, 5  $\mu$ m.



with bead pseudotargets. If two cells with freely diffusible homophilic membrane proteins were to touch, we would expect *trans*-dimers to concentrate in the region of overlap over time. In fact, apCAM does concentrate at such overlap regions (Fig. 1C). In our bead experiments, as apCAM concentration increases, the protein transits from a freely diffusible state, to an F-actin coupled state, then eventually triggers actin polymerization. We would therefore expect interacting neurons to transit through these three behaviors over time, as apCAM concentrates in the overlap region. During such interactions, growth cones initially overlap, but do not appear to react to each other. After a variable amount of time in contact, growth cone lamellae exert retrograde flow dependent tension on each other, that appears to result from coupling of the two growth cones' actin cytoskeletons. Finally, active membrane ruffling and growth occurs at the contact site, suggestive of stimulated F-actin polymerization (Lin and Forscher, 1993; Lin and Forscher, 1995). The parallel sequence of events observed in bead studies and growth cone-target interactions suggest similar pathways may be involved.

Particles derivatized with integrin or NCAM antibodies have previously been used to investigate membrane protein mobility and cytoskeletal interaction in both fibroblasts and neurons (Sheetz et al., 1990; Schmidt et al., 1993, 1995). In these reports particles tended to diffuse extensively, and sometimes exhibited rapid directed excursions, usually towards the leading edge of cells. In addition, in neurons, integrin binding particles appeared to be preferentially associated with the leading edge of the growth cone. The inductopodia associated motility reported here appears to be distinct from the particle behavior observed in the above studies, having only a limited diffusional component, slower instantaneous velocity, and does not appear to occur with greater efficacy in a particular portion of the lamellipodium.

Interestingly, several intracellular bacterial pathogens, including *Listeria monocytogenes*, *Shigella flexneri* and *Vaccinia* virus (Dabiri et al., 1990; Theriot et al., 1992; Kadurugamuwa et al., 1991; Cudmore et al., 1995) have been shown to utilize site directed actin assembly as a propulsive mechanism in the host cell and as a means of intercellular infection. All of these pathogens assemble F-actin tail structures which appear morphologically identical to inductopodia. In the bacterial examples, actin assembly has been shown to be coordinated by a complex of identified bacterial and host cell proteins (Bernardini et al., 1989; Kocks et al., 1992). Inductopodia differ in that stimulation of actin assembly occurs across the plasma membrane instead of at the pathogen surface in the host cell cytoplasm, and does not rely on exogenous proteins. It is tempting to speculate that apCAM recruits a protein complex analogous to that used by the pathogens above. The striking similarity of the resulting actin polymerization driven transport in such diverse cell types suggests utilization of a conserved physiological process potentially underlying phenomena such as membrane ruffling, filopodial extension, phagocytosis and dendritic spine remodeling in neurons.

The authors thank Drs William Bement, Richard Cheney, Joseph Wolenski and Laura Errante for valuable comments and suggestions, and Drs Flavio Keller and Sam Schacher for the monoclonal antibody 4E8. This work was supported by National Institutes of Health grant

NS28695 and an award from the McKnight Endowment Fund for Neuroscience to P.F.; a fellowship from the Department of Education of Taiwan to C.-H.L. and NIH Training Grant T32GM07223 to C.T.

## REFERENCES

- Ambron, R. T., Protic, J., Den, H. and Gabel, C. A.** (1989). Identification of protein-bound oligosaccharides on the surface of growth cones that bind to muscle cells. *J. Neurobiol.* **20**, 549-568.
- Atashi, J. R., Klinz, S. G., Ingraham, C. A., Matten, W. T., Schachner, M. and Maness, P. F.** (1992). Neural cell adhesion molecules modulate tyrosine phosphorylation of tubulin in nerve growth cone membranes. *Neuron* **8**, 831-842.
- Bailey, C. H., Chen, M., Keller, F. and Kandel, E. R.** (1992). Serotonin-mediated endocytosis of apCAM: An early step of learning-related synaptic growth in *Aplysia*. *Science* **256**, 645-649.
- Bernardini, M. L., Mounier, J., D'Hauteville, H., Coquis-Rondon, M. and Sansonetti, P. J.** (1989). Identification of icsA, a plasmid locus of *Shigella flexneri* that governs bacterial intra- and intercellular spread through interaction with F-actin. *Proc. Nat. Acad. Sci. USA* **86**, 3867-3871.
- Bixby, J. L. and Harris, W. A.** (1991). Molecular mechanisms of axon growth and guidance. *Annu. Rev. Cell Biol.* **7**, 117-159.
- Block, S. M.** (1990). Optical tweezers: a new tool for biophysics. In *Noninvasive Techniques in Cell Biology* (ed. J. K. Foskett and S. Grinstein), pp. 375-402. Wiley-Liss, New York.
- Carpen, O., Pallai, P., Staunton, D. E. and Springer, T. A.** (1992). Association of intercellular adhesion molecule-1 (ICAM-1) with actin-containing cytoskeleton and alpha-actinin. *J. Cell Biol.* **118**, 1223-1234.
- Cudmore, S., Cossart, P., Griffiths, G. and Way, M.** (1995). Actin-based motility of vaccinia virus. *Nature* **378**, 636-638.
- Dabiri, G. A., Sanger, J. M., Portnoy, D. A. and Southwick, F. S.** (1990). *Listeria monocytogenes* moves rapidly through the host-cell cytoplasm by inducing directional actin assembly. *Proc. Nat. Acad. Sci. USA* **87**, 6068-6072.
- Davis, J. Q., McLaughlin, T. and Bennett, V.** (1993). Ankyrin-binding proteins related to nervous system cell adhesion molecules: candidates to provide transmembrane and intercellular connections in adult brain. *J. Cell Biol.* **121**, 121-133.
- Doherty, P., Cohen, J. and Walsh, F. S.** (1990a). Neurite outgrowth in response to transfected N-CAM changes during development and is modulated by polysialic acid. *Neuron* **5**, 209-219.
- Doherty, P., Fruns, M., Seaton, P., Dickson, G., Barton, C. H., Sears, T. A. and Walsh, F. S.** (1990b). A threshold effect of the major isoforms of NCAM on neurite outgrowth. *Nature* **343**, 464-466.
- Doherty, P., Ashton, S. V., Moore, S. E. and Walsh, F. S.** (1991). Morphoregulatory activities of NCAM and N-cadherin can be accounted for by G protein-dependent activation of L- and N-type neuronal Ca channels. *Cell* **67**, 21-33.
- Doherty, P., Rowett, L. H., Moore, S. E., Mann, D. A. and Walsh, F. S.** (1991). Neurite outgrowth in response to transfected N-CAM and N-cadherin reveals fundamental differences in neuronal responsiveness to CAMS. *Neuron* **6**, 247-258.
- Doherty, P., Moolenaar, C. E., Ashton, S. V., Michalides, R. J. and Walsh, F. S.** (1992). The VASE exon downregulates the neurite growth-promoting activity of NCAM 140. *Nature* **356**, 791-793.
- Forscher, P., Kaczmarek, L. K., Buchanan, J. and Smith, S. J.** (1987). Cyclic AMP induced changes in distribution and transport of organelles within growth cones of *Aplysia* bag cell neurons. *J. Neurosci.* **7**, 3600-3611.
- Forscher, P. and Smith, S. J.** (1988). Actions of the cytochalasins on the organization of actin filaments and microtubules in a neuronal growth cone. *J. Cell Biol.* **107**, 1505-1516.
- Forscher, P. and Smith, S. J.** (1990). Cytoplasmic actin filaments move particles on the surface of a neuronal growth cone. In *Optical Microscopy for Biology* (ed. B. Herman and K. Jacobson), pp. 459-471. Wiley Liss, Inc., New York.
- Forscher, P., Lin, C. H. and Thompson, C.** (1992). Novel form of growth cone motility involving site-directed actin filament assembly. *Nature* **357**, 515-518.
- Gumbiner, B. M.** (1993). Proteins associated with the cytoplasmic surface of adhesion molecules. *Neuron* **11**, 551-564.
- Hall, A. K., Nelson, R. and Rutishauser, U.** (1990). Binding properties of detergent-solubilized NCAM. *J. Cell Biol.* **110**, 817-824.

- Harrelson, A. L. and Goodman, C. S.** (1988). Growth cone guidance in insects: Fasciclin II is a member of the immunoglobulin superfamily. *Science* **242**, 700-708.
- Holifield, B. F., Ishihara, A. and Jacobson, K.** (1990). Comparative behavior of membrane protein-antibody complexes on motile fibroblasts: implications for a mechanism of capping. *J. Cell Biol.* **111**, 2499-2512.
- Holifield, B. F. and Jacobson, K.** (1991). Mapping trajectories of Pgp-1 membrane protein patches on surfaces of motile fibroblasts reveals a distinct boundary separating capping on the lamella and forward transport on the retracting tail. *J. Cell Sci.* **98**, 191-203.
- Kadurugamuwa, J. L., Rohde, M., Wehland, J. and Timmis, K. N.** (1991). Intercellular spread of *Shigella flexneri* through a monolayer mediated by membranous protrusions and associated with reorganization of the cytoskeletal protein vinculin. *Infect. Immunol.* **59**, 3463-3471.
- Keller, F. and Schacher, S.** (1990). Neuron-specific membrane glycoproteins promoting neurite fasciculation in *Aplysia californica*. *J. Cell Biol.* **111**, 2637-2650.
- Kocks, C., Gouin, E., Tabouret, M., Berche, P., Ohayon, H. and Cossart, P.** (1992). L. monocytogenes-induced actin assembly requires the actA gene product, a surface protein. *Cell* **68**, 521-531.
- Lemmon, V., Farr, K. L. and Lagenaur, C.** (1989). L1-mediated axon outgrowth occurs via a homophilic binding mechanism. *Neuron* **2**, 1597-1603.
- Letourneau, P. C.** (1987). What happens when growth cones meet neurites: Attraction or repulsion? *Trends Neurosci.* **10**, 390-392.
- Letourneau, P. C., Shattuck, T. A. and Ressler, A. H.** (1987). 'Pull' and 'push' in neurite elongation: Observations on the effects of different concentrations of cytochalasin-B and taxol. *Cell Motil. Cytoskel.* **8**, 193-209.
- Lin, C.-H. and Forscher, P.** (1993). Cytoskeletal remodeling during growth cone-target interactions. *J. Cell Biol.* **121**, 1369-1383.
- Lin, C.-H., Thompson, C. A. and Forscher, P.** (1994). Cytoskeletal reorganization underlying growth cone motility. *Curr. Opin. Neurobiol.* **4**, 640-647.
- Lin, C.-H. and Forscher, P.** (1995). Growth cone advance is inversely proportional to retrograde F-actin flow. *Neuron* **14**, 763-771.
- Mayford, M., Barzilai, A., Keller, F., Schacher, S. and Kandel, E. R.** (1992). Modulation of an NCAM-related adhesion molecule with long-term synaptic plasticity in *Aplysia*. *Science* **256**, 638-644.
- Neugebauer, K. M., Tomaselli, K. J., Lilien, J. and Reichardt, L. F.** (1988). N-cadherin, NCAM and integrins promote retinal neurite outgrowth on astrocytes in vitro. *J. Cell Biol.* **107**, 1177-1187.
- Peter, N., Aronoff, B., Wu, F. and Schacher, S.** (1994). Decrease in growth cone-neurite fasciculation by sensory or motor cells in vitro accompanies downregulation of *Aplysia* cell adhesion molecules by neurotransmitters. *J. Neurosci.* **14**, 1413-21.
- Pollerberg, G. E., Schachner, M. and Davoust, J.** (1986). Differentiation state-dependent surface mobilities of two forms of the neural cell adhesion molecule. *Nature* **324**, 462-465.
- Pollerberg, G. E., Burridge, K., Krebs, K. A., Goodman, S. R. and Schachner, M.** (1987). The 180-kD component of the neural cell adhesion molecule N-CAM is involved in cell-cell contacts and cytoskeleton-membrane interactions. *Cell Tissue Res.* **250**, 227-236.
- Qian, H., Sheetz, M. P. and Elson, E. L.** (1991). Single particle tracking: analysis of diffusion in two-dimensional systems. *Biophys. J.* **60**, 910-921.
- Schmidt, C. E., Horwitz, A. F., Lauffenburger, D. A. and Sheetz, M. P.** (1993). Integrin-cytoskeletal interactions in migrating fibroblasts are dynamic, asymmetric, and regulated. *J. Cell Biol.* **123**, 977-991.
- Schmidt, C. E., Dai, J., Lauffenburger, D. A., Sheetz, M. P. and Horwitz, A. F.** (1995). Integrin-cytoskeletal interactions in neuronal growth cones. *J. Neurosci.* **15**, 3400-3407.
- Sheetz, M. P., Turney, S., Qian, H. and Elson, E.** (1989). Nanometre-level analysis demonstrates that lipid flow does not drive membrane glycoprotein movements. *Nature* **340**, 284-288.
- Sheetz, M. P., Baumrind, N. L., Wayne, D. B. and Pearlman, A. L.** (1990). Concentration of membrane antigens by forward transport and trapping in neuronal growth cones. *Cell* **61**, 231-241.
- Shiozawa, J. A., Brandts, J. F. and Jacobson, B. S.** (1989). Binding of plasma membrane glycoproteins to the cytoskeleton during patching and capping is consistent with an entropy-enhancement model. *Biochim. Biophys. Acta* **980**, 361-366.
- Svoboda, K. and Block, S. M.** (1994). Biological applications of optical forces. *Annu. Rev. Biophys. Biomol. Struct.* **23**, 247-285.
- Tanaka, E. and Sabry, J.** (1995). Making the connection: cytoskeletal rearrangements during growth cone guidance. *Cell* **83**, 171-176.
- Theriot, J. A., Mitchison, T. J., Tilney, L. G. and Portnoy, D. A.** (1992). The rate of actin-based motility of intracellular *Listeria monocytogenes* equals the rate of actin polymerization. *Nature* **357**, 257-260.
- Wheelock, M. J. and Knudsen, K. A.** (1991a). Cadherins and associated proteins. *In Vivo* **5**, 505-513.
- Wheelock, M. J. and Knudsen, K. A.** (1991b). N-cadherin-associated proteins in chicken muscle. *Differentiation* **46**, 35-42.
- Zhu, H., Wu, F. and Schacher, S.** (1995). Changes in expression and distribution of *Aplysia* cell adhesion molecules can influence synapse formation and elimination in vitro. *J. Neurosci.* **15**, 4173-83.

(Received 20 June 1996 - Accepted 5 September 1996)